**SUPPORTING INFORMATION**

# Circulation Time-optimized Albumin Nanoplatform for Quantitative Visualization of Lung Metastasis via Targeting of Macrophages

Hyewon Chung,[1,2,‡] Ji Yong Park,[3,4,5,6‡] Kyuwan Kim,[4,5] Ran Ji Yoo,[4,5] Minseok Suh,[7] Gyo Jeong Gu,[1] Jin Sil Kim,[4] Tae Hyeon Choi,[4,7] Jung Woo Byun,[4] Young Wook Ju,[8] Wonshik Han,[8] Han Suk Ryu,[9] Gehoon Chung,[6,10] Do Won Hwang,[4,11] Yujin Kim,[3] Hye-Ryun Kang,[3] Yi Rang Na,[12] Hongyoon Choi,[4] Hyung-Jun Im,[7,13] Yun-Sang Lee,[3,4,5,*] Seung Hyeok Seok[1,3,*]

[1]Macrophage Lab, Department of Microbiology and Immunology, and Institute of Endemic Disease, Seoul National University College of Medicine, Seoul 03080, Republic of Korea

[2]Bio-MAX Institute, Seoul National University, Seoul 03080, Republic of Korea

[3]Department of Biomedical Sciences, Seoul National University Graduate School, Seoul 03080, Republic of Korea

[4]Department of Nuclear Medicine, Seoul National University Hospital, Seoul 03080, Republic of Korea

[5]Cancer Research Institute, Seoul National University, Seoul 03080, Republic of Korea

[6]Dental Research Institute, Seoul National University, Seoul 03080, Republic of Korea

[7]Department of Molecular Medicine and Biopharmaceutical Sciences, Graduate School of Convergence Science and Technology, Seoul National University; Seoul, Republic of Korea

[8]Department of Surgery and Cancer Research Institute, Seoul National University College of Medicine, Seoul 03080, Republic of Korea

[9]Department of Pathology, Seoul National University College of Medicine, Seoul 03080, Republic of Korea

[10]Department of Oral Physiology, Seoul National University, School of Dentistry, Seoul 03080, Republic of Korea

[11]Research and Development Center, THERABEST, Co. Ltd., Seoul, Korea

[12]Transdisciplinary Department of Medicine and Advanced Technology, Seoul National University Hospital, Seoul 03080, Republic of Korea

[13]Research Institute for Convergence Science, Seoul National University; Seoul, 08826, Republic of Korea

[‡]These authors contributed equally.

**A Reaction mechanism**

1. Albumin reaction with ADIBO-NHS

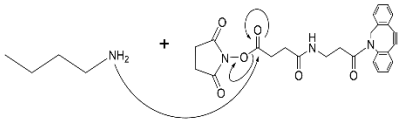

2. ADIBO-Albumin reaction
with Azide functionalized compound (Click reaction)

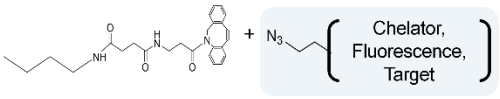


3. Mannosylated albumin (Man-Alb)
with radioisotope & fluorescence (FL)

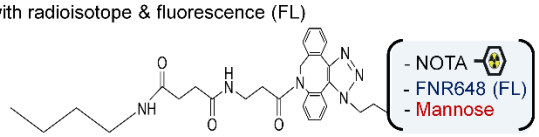


**B Equations for calculating of UV based measurement**

**Equation 1.** $A_{280c} = A_{280} - A_{309} \times CF$

Measured absorbance of albumin: $A_{280}$
Measured absorbance of ADIBO: $A_{309}$
Corrected absorbance of albumin: $A_{280c}$
Correction factor (CF) = 0.8658

**Equation 2.**
**Absorbance = ε ($M^{-1}cm^{-1}$) x concentration (mol/L) x length (cm)**

**Equation 3.** $DOF = [(A_{309}/\varepsilon_{309,\ ADIBO})/(A_{280c}/\varepsilon_{280,\ Albumin})]$

$\varepsilon_{309,\ ADIBO}$ ($M^{-1}cm^{-1}$) = 12000
$\varepsilon_{280,\ Albumin}$ ($M^{-1}cm^{-1}$) = 35295.5
Concentration of albumin (mol/L) = $A_{280c}$ / ($\varepsilon_{280,\ Albumin}$ x length)
Concentration of ADIBO (mol/L) = $A_{309}$/ ($\varepsilon_{309,\ ADIBO}$ x length)
DOF: Degree of functionalization (= Number of ADIBO per albumin)

**Supplementary Figure 1. Synthesis of RI-Man-Alb-FL.** (A) Reaction mechanism and flow of clickable modification on albumin. (B) Equation for calculating the ADIBO number on albumin.

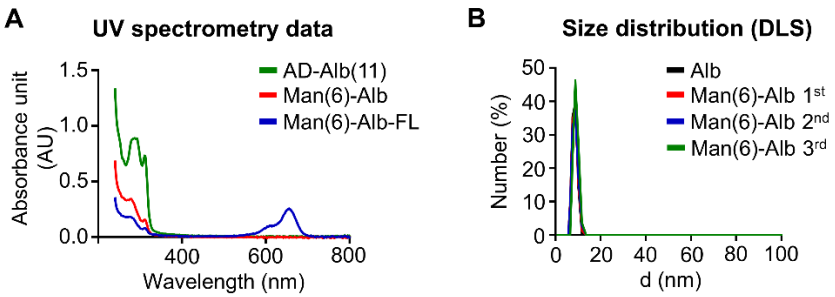


4

5 **Supplementary Figure 2. UV spectra and size of albumins.** (A) The concentrations used in the

6 experiments were confirmed using UV spectroscopy. (B) The size of Man(6)-Alb measured using

7 DLS.

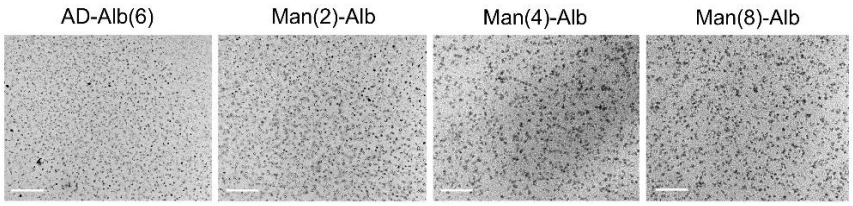


**Supplementary Figure 3. TEM images of AD-Alb(6), Man(2)-Alb, Man(4)-Alb and Man(8)-Alb.** Scale bar = 500 nm.

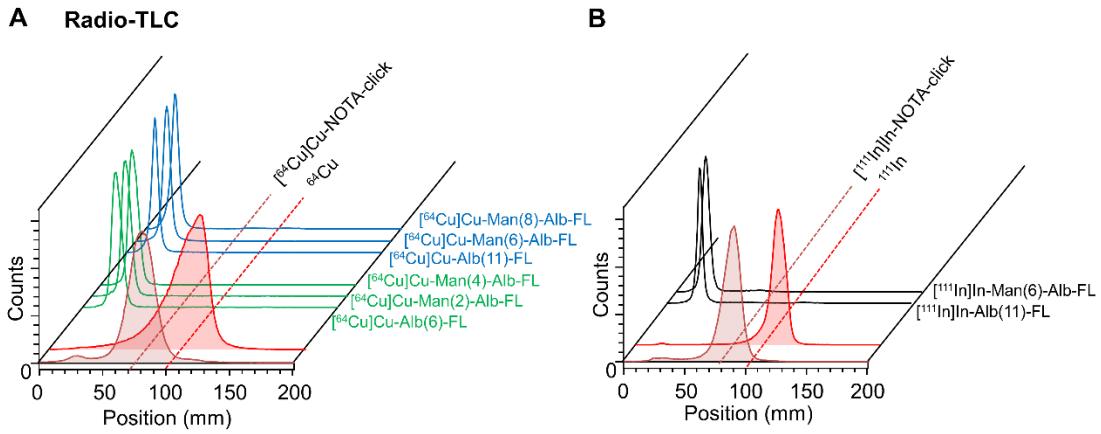


**Supplementary Figure 4. Labeling efficiency of all the MSAs used in experiments.** Labeling of each MSAs was assessed after click reaction with $^{64}$Cu-NOTA-$N_3$ (A) and $^{111}$In-NOTA-$N_3$ (B). The radiochemical purity was determined using radio TLC chromatogram and percentage of value at $R_f$ = 0.0 ~ 0.1.

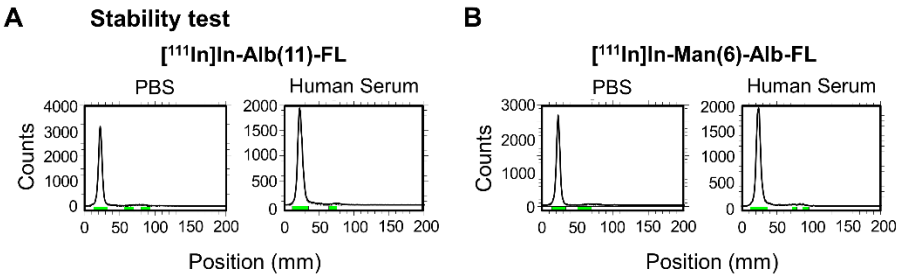


16

17 **Supplementary Figure 5. Labeling stability of Alb(11)-FL and Man(6)-Alb-FL.** The

18 radiochemical purity of Alb(11)-FL (A) and Man(6)-Alb-FL (B) was assessed after $^{111}$In

19 radiolabeling using radio TLC chromatogram and percentage of value at $R_f$ = 0.0 ~ 0.1.

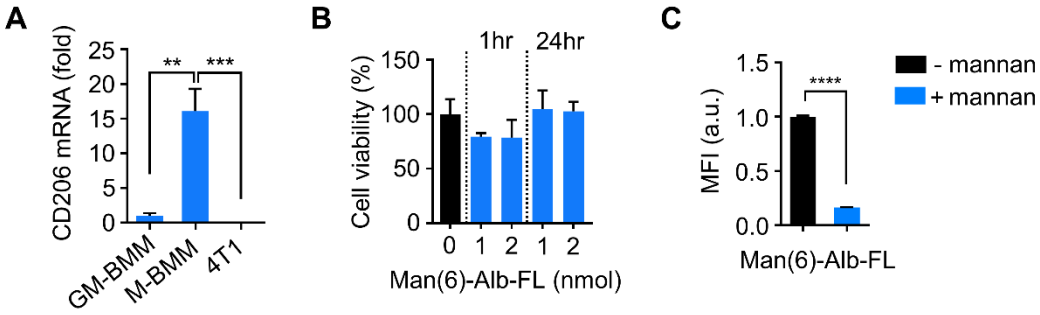


20

21 **Supplementary Figure 6. *In vitro* CD206-specific uptake of Man(6)-Alb-FL in macrophages.**

22 (A) CD206 mNRA expression in GM-BMM, M-BMM, and 4T1 cells. n = 4 ~ 6 /group. (B) M-BMM

23 cell viability after incubation with various concentrations of Man(6)-Alb-FL for 1 or 24 hr. n =

24 3/group. (C) Blocking of Man(6)-Alb-FL uptake by mannan pretreatment. M-BMMs were pre-

25 incubated with or without mannan before the addition of Man(6)-Alb-FL and then uptake was

26 measured using flow cytometry after incubation with Man(6)-Alb-FL for 1 h. n = 5 ~ 6 /group. Data

27 show means ± SEM. $^{**}P < 0.01$, $^{***}P < 0.001$, $^{****}P < 0.0001$ using Student's t-test.

A

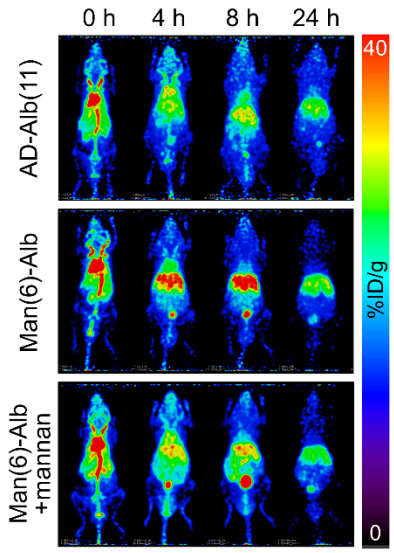


B

AD-Alb(11)

| Time | Blood pool (%ID/g) | | Liver (%ID/g) | | Lung (%ID/g) | |
|---|---|---|---|---|---|---|
| | Average | SD | Average | SD | Average | SD |
| 0 h | 45.11 | 1.47 | 16.54 | 1.2 | 9.76 | 2.77 |
| 4 h | 28.68 | 1.84 | 22.8 | 1.9 | 5.65 | 0.87 |
| 8 h | 22.46 | 1.4 | 25.87 | 1.7 | 3.7 | 0.75 |
| 24 h | 12.09 | 0.9 | 20.34 | 2.4 | 2.56 | 0.22 |

Man(6)-Alb

| Time | Blood pool (%ID/g) | | Liver (%ID/g) | | Lung (%ID/g) | |
|---|---|---|---|---|---|---|
| | Average | SD | Average | SD | Average | SD |
| 0 h | 46.48 | 2.08 | 20.01 | 2.8 | 9.32 | 1.98 |
| 4 h | 24.85 | 2.11 | 38.12 | 1.9 | 4.86 | 0.65 |
| 8 h | 15.12 | 1.75 | 45.66 | 1.65 | 2.99 | 0.53 |
| 24 h | 2.41 | 0.23 | 22.65 | 3.25 | 1.06 | 0.32 |

Man(6)-Alb + mannan

| Time | Blood pool (%ID/g) | | Liver (%ID/g) | | Lung (%ID/g) | |
|---|---|---|---|---|---|---|
| | Average | SD | Average | SD | Average | SD |
| 0 h | 47.69 | 3.8 | 14.98 | 2.6 | 9.55 | 2.12 |
| 4 h | 27.54 | 2.3 | 24.54 | 2.51 | 5.02 | 0.95 |
| 8 h | 20.98 | 1.89 | 26.97 | 2.02 | 3.13 | 0.55 |
| 24 h | 2.81 | 0.57 | 21.98 | 2.9 | 1.2 | 0.22 |

**Supplementary Figure 7. *In vivo* PET imaging of [$^{64}$Cu]Cu-Man(6)-Alb-FL after treatment with mannan in tumor-free mice.** (A) PET images of tumor-free mice acquired 0, 4, 8 and 24 h post-injection of [$^{64}$Cu]Cu-AD(11)-FL, [$^{64}$Cu]Cu-Man(6)-Alb-FL or [$^{64}$Cu]Cu-Man(6)-Alb-FL with a blocking dose of mannan (blocking group). (B) Quantification of signals in the blood, liver and lung measured using PET imaging. n = 4 mice/group.

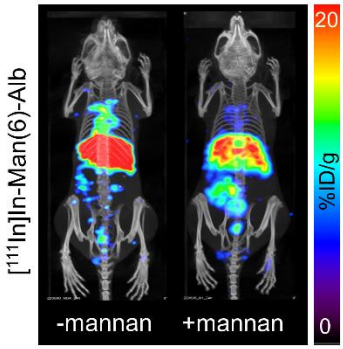


**Supplementary Figure 8.** ***In vivo*** **SPECT/CT imaging of [$^{111}$In]In-Man(6)-Alb-FL after treatment with mannan in tumor-bearing mice.** SPECT/CT images of 4T1 tumor-bearing mice acquired 24 h post-injection of [$^{111}$In]In-Man(6)-Alb-FL or [$^{111}$In]In-Man(6)-Alb-FL with a blocking dose of mannan (blocking group). n = 4/group.

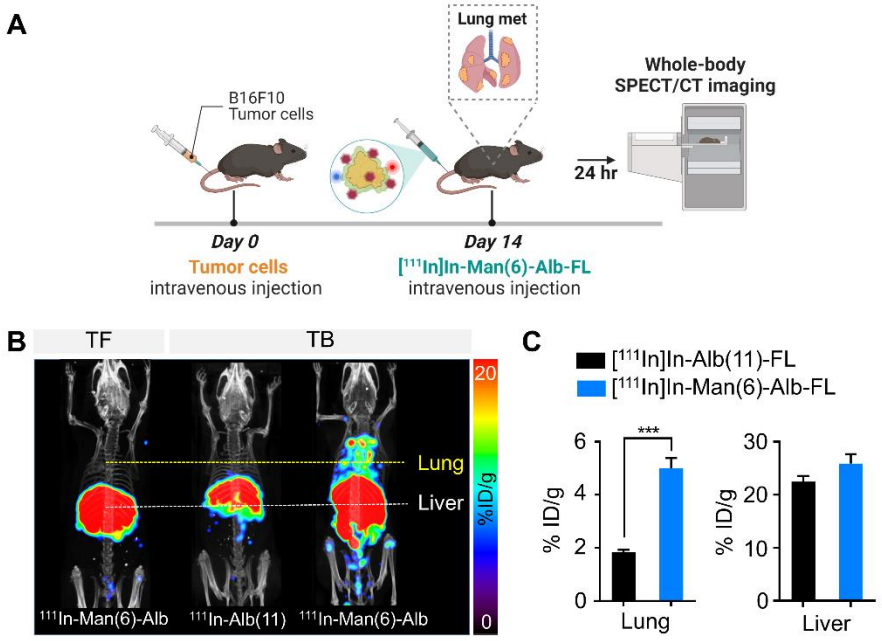


**Supplementary Figure 9. [$^{111}$In]In-Man(6)-Alb-FL noninvasively visualizes metastatic lesions in lungs in B16F10 melanoma-bearing mice.** (A) Schematic of the experiment showing intravenous injection of B16F10 cells, followed by intravenous injection of [$^{111}$In]In-Man(6)-Alb-FL and SPECT/CT imaging. (B) MIP SPECT/CT images of tumor-free (TF) and B16F10-bearing mice (TB) 24 h after injection with [$^{111}$In]In-Alb(11)-FL or [$^{111}$In]In-Man(6)-Alb-FL. (C) Quantification of [$^{111}$In]In-Alb(11)-FL or [$^{111}$In]In-Man(6)-Alb-FL in the lungs and livers of the B16F10-bearing mice, expressed as % ID/g. n = 5 mice/group. Data show means ± SD. ***$P < 0.001$ using Student's t-test.

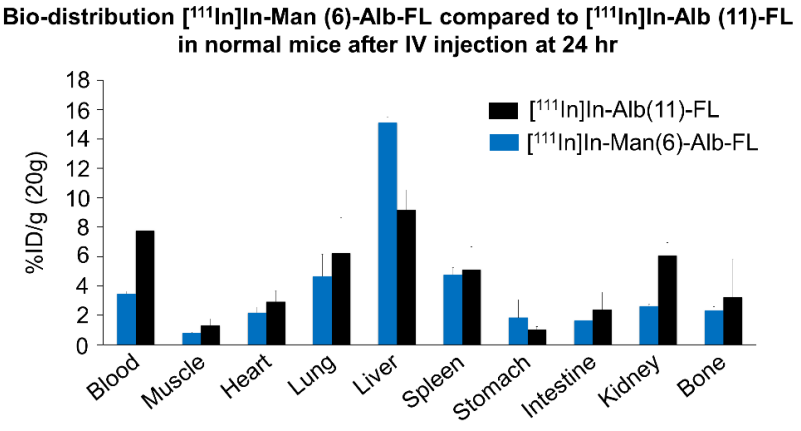


48

49 **Supplementary Figure 10.** ***Ex vivo*** **biodistribution of [$^{111}$In]In-Alb(11)-FL and [$^{111}$In]In-**

50 **Man(6)-Alb-FL 24 h after injection.** Comparison between [$^{111}$In]In-Alb(11)-FL and [$^{111}$In]In-

51 Man(6)-Alb-FL in normal mice 24 h after injection.

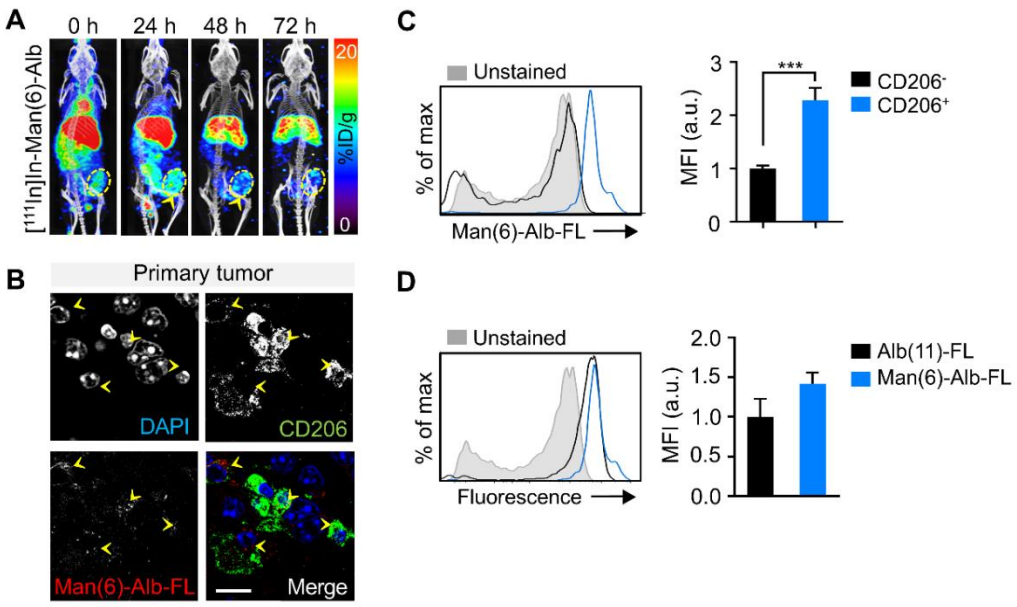


**Supplementary Figure 11. CD206-specific uptake of [$^{111}$In]In-Man(6)-Alb-FL in primary tumor**. (A) 4T1-bearing mice (day 14) were injected with [$^{111}$In]In-Man(6)-Alb-FL and SPECT/CT images were obtained at 3, 24, 48, and 72 h. Signal in tumor (yellow arrowheads) increased until the first day, after which the overall signal weakened, including that in the liver. (B) Representative confocal immunofluorescent images showing *in vivo* localization of injected Man(6)-Alb-FL (red) and CD206$^+$ macrophages (green) within the tumors from 4T1-bearing mice (day 28). The yellow arrowheads indicate CD206$^+$ macrophage-specific Man(6)-Alb-FL uptake. DAPI, blue. Scale bar =10 μm. (C, D) Quantification of CD206$^+$ macrophage-specific Man(6)-Alb-FL uptake *in vivo* was analyzed using flow cytometry. (C) Man(6)-Alb-FL uptake by each gated CD206$^-$ macrophage (CD45$^+$CD11b$^+$F4/80$^+$CD206$^-$) and CD206$^+$ macrophage (CD45$^+$CD11b$^+$F4/80$^+$CD206$^+$) subset as determined by fold change in mean fluorescence intensity (MFI) of co-labeled fluorescent dye (FNR-648). (D) Fold change in MFI of co-labeled FNR-648 on CD206$^+$ macrophage from 4T1-bearing mice following injection with Alb(11)-FL or Man(6)-Alb-FL. n = 5 ~ 7 mice/group. Data show means ± SEM. ***$P < 0.001$ using Student's t-test.

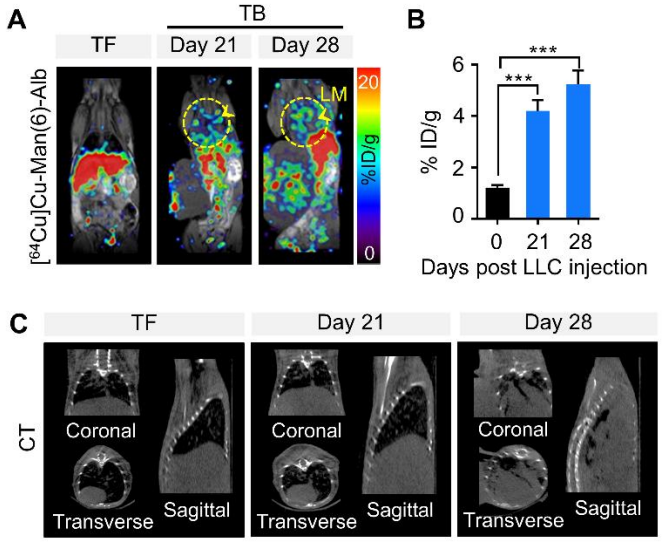


**Supplementary Figure 12.** ***In vivo*** **[$^{64}$Cu]Cu-Man(6)-Alb-FL imaging of lung metastases in LLC tumor-bearing mice.** Simultaneous PET/MRI imging of [$^{64}$Cu]Cu-Man(6)-Alb-FL (A, B) and CT imaging (C) were performed in tumor-free (TF, control) and LLC-bearing mice (TB) on days 21 and 28. (A) Representative PET/MRI images of [$^{64}$Cu]Cu-Man(6)-Alb-FL. Strong signal was observed in the metastatic lung (LM, yellow arrowheads). (B) Quantification of [$^{64}$Cu]Cu-Man(6)-Alb-FL signal in the resected lung, expressed as % ID/g. (C) CT images (coronal, transverse, and sagittal views) are also shown. Representative CT images show strong signals from lung metastases on day 28, while no significant change was detected at an earlier stage (day 21). n = 4 mice/group. Data represent mean ± SEM. ***$P$ < 0.001 using Student's t-test.

A

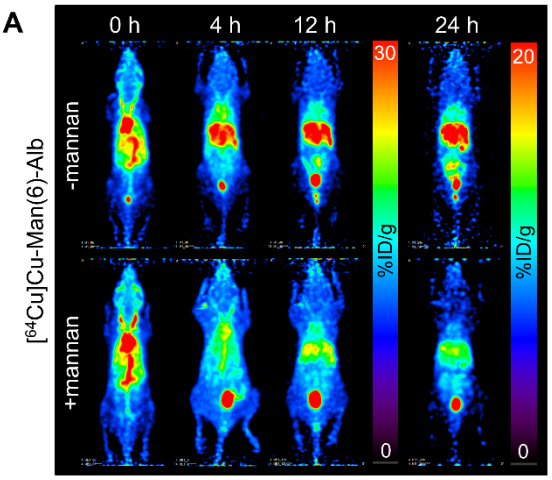


B

Man(6)-Alb

| Time | Blood pool (%ID/g) | | Liver (%ID/g) | | Lung (%ID/g) | |
|---|---|---|---|---|---|---|
| | Average | SD | Average | SD | Average | SD |
| 0 h | 43.22 | 2.87 | 13.21 | 2.5 | 8.58 | 2.17 |
| 4 h | 22.87 | 1.33 | 28.34 | 2 | 6.95 | 0.31 |
| 12 h | 14.2 | 1.24 | 33.12 | 1.8 | 6.23 | 0.4 |
| 24 h | 2.31 | 0.23 | 20.24 | 2.94 | 5.51 | 0.22 |

Man(6)-Alb + mannan

| Time | Blood pool (%ID/g) | | Liver (%ID/g) | | Lung (%ID/g) | |
|---|---|---|---|---|---|---|
| | Average | SD | Average | SD | Average | SD |
| 0 h | 44.87 | 3.13 | 12.34 | 2.77 | 8.76 | 1.96 |
| 4 h | 25.65 | 2.59 | 15.32 | 1.99 | 4.87 | 0.83 |
| 12 h | 12.9 | 1.85 | 18.2 | 2.21 | 2.97 | 0.33 |
| 24 h | 2.22 | 0.33 | 9.73 | 1.32 | 1.63 | 0.15 |

**Supplementary Figure 13.** ***In vivo*** **PET imaging of [$^{64}$Cu]Cu-Man(6)-Alb-FL after treatment with mannan in 4T1 tumor-bearing mice.** (A) PET images of 4T1 tumor-bearing mice acquired 0, 4, 12 and 24 h post-injection of [$^{64}$Cu]Cu-Man(6)-Alb-FL or [$^{64}$Cu]Cu-Man(6)-Alb-FL with a blocking dose of mannan (blocking group). (B) Quantification of [$^{64}$Cu]Cu-Man(6)-Alb-FL in the blood, liver and lung of the 4T1-bearing mice measured using PET imaging. n = 4 ~ 5/group.

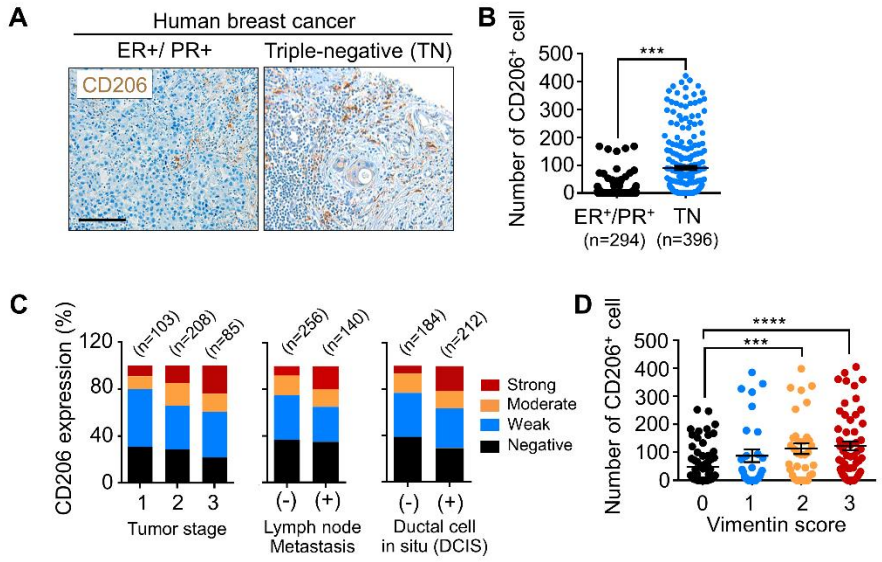


**Supplementary Figure 14. Strong correlation between CD206 expression and metastatic potential in human breast tumor tissues.** (A, B) Representative images of CD206 staining in tissue microarray (A) and quantification of $CD206^+$ cells (B) in tumor tissues from $ER^+/PR^+$ breast cancer patients (n = 294) and triple-negative (TN) breast cancer patients (n = 396). Scale bar = 500 nm. (C, D) The correlation between CD206 expression and tumor stage (C, left panel), lymph node metastasis (C, middle panel), ductal cell *in situ* (DCIS) (C, right panel), and tumor vimentin score (D) in tumor tissues from TN breast cancer patients. Data represent mean ± SEM. ***$P < 0.001$, ****$P < 0.0001$ using Student's t-test.